H13-31

POLLUTANT TRANSFER COEFFICIENT IN STREET CANYONS OF DIFFERENT ASPECT RATIOS USING LARGE-EDDY SIMULATION AND *k-ε* TURBULENCE MODEL

Tracy N.H. Chung and Chun-Ho Liu

Department of Mechanical Engineering, The University of Hong Kong, Pokfulam Road, Hong Kong

Abstract: To enrich our understanding of the flow and pollutant removal in urban areas, the wind and pollutant transport in idealized two-dimensional (2D) street canyons of building-height-to-street-width (aspect) ratios (ARs) 0.0667, 0.0909, and 0.25 were simulated by both the Reynolds-averaged Navier-Stokes (RANS) equations with the renormalization group (RNG) *k-ε* turbulence model and the large-eddy simulation (LES) with the one-equation subgrid-scale (SGS) model. To examine the pollutant removal performance, the local convective pollutant transfer coefficient (LPTC) is depicted as a spatial function on the ground of the street canyons. In the isolated roughness regime (ARs = 0.0667 or 0.0909), persistent flow reattachment and separation are observed inside the street canyons. It is found that the LPTC is tightly coupled with the flow recirculations in which the maximum and minimum LPTC coincide, respectively, with the points of reattachment and separation. In the wake interference regime (AR = 0.25), both reattachment and separation diminish that ends up with only one primary recirculation in the narrower street canyon. Instead of peaks and troughs, the LPTC is monotonic that is higher on the windward side. Apart from the ground-level LPTC, analysis of the roof-level pollutant transport signifies that in the isolated roughness regime the pollutant removal is mainly governed by the fresh air entrainment from the shear layer down into the street canyons. While in the wake interference regime, turbulent dispersion dominates the pollutant removal. The comparison among the experimental and modelling results demonstrates that the LES is more accurately resolving LPTC especially under the strong shear along the interface in-between recirculations.

Key words: *Large-eddy simulation; k-ε turbulence model; Isolated roughness regime; Wake interference regime; Local transfer coefficient*

INTRODUCTION

In view of the adverse impact of poor air quality on human health (WHO, 2007) and the economy across the world, air pollution, especially in urban areas, is an international issue which cannot be overlooked anymore. A number of studies have been performed to study the effects of building geometries on atmospheric flows for decades. Field measurements (Berkowicz *et al.*, 2002), wind tunnel experiments (Barlow *et al.*, 2004), and numerical simulations (Letzel *et al.*, 2008) are the three most typical research methods nowadays. A street canyon is the generic two-dimensional (2D) structure most commonly used in urban climate research. Its building-height-to-street-width ratio (h/b), also known as aspect ratio (AR), is the key geometry parameter defining the building configuration and the flow pattern as well. Three characteristic flow regimes, including isolated roughness (AR < 0.3), wake interference (0.3 < AR < 0.7), and skimming (0.7 < AR), have been distinguished by Oke (1988). Temperature, which is often taken as a passive scalar in heat transfer, is closely coupled to the flow characteristics. Numerous studies have been performed to examine the dependence between flows and convective heat transfer (Liou *et al.*, 1993; Acharya *et al.*, 1993) however, the investigations of the mass (pollutant) transfer counterpart in turbulence are rather limited. In this paper, as a pilot study, we focus on the correlation between the flow characteristics and the pollutant removal performance in a 2D idealized urban street canyon in turbulent flow.

THEORETICAL BACKGROUND

As shown in Aliaga *et al.* (1994), the flow regime has direct effect on the temperature distribution in 2D ribs placed in cross flow (the street canyon counterpart in heat transfer). In the isolated roughness regime, the local heat transfer coefficient (LHTC) exhibits a tight coupling with the flow reattachment and separation. In the wake interference regime, the spatial behaviour of LHTC is governed by the primary recirculation. Consistently findings were also reported in Hishida (1996).

In the isolated roughness regime, the local Nusselt number (Nu) attains its maximum near the reattachment on the leeward side of the street canyon. This peak is the result of the fresh air impingement on the street, signifying the more effective heat transfer from the ground to the prevalent flow aloft. After the reattachment, the entraining air stream develops a boundary layer and a wall jet, respectively, on the leeward and windward sides. The boundary layer reduces the LHTC until the secondary recirculation on the windward side, where the flow separation promotes the heat transfer rapidly developing another local maximum. At the same time, the downward wall jet along the windward facade impinges near the ground-level windward contributing to the trough of LHTC in the separation region in the secondary recirculation in counter flow.

In the wake interference regime, the LHTC is monotonically increasing from the leeward side to the windward side. Different from the isolated roughness region, only one primary recirculation is developed in the narrower street canyon. The air stream entrains into the street canyon near the windward facade. The impingement on the ground then initiates a wall jet flowing reversely to the leeward side. Similar to that in the isolated roughness regime, the impingement rapidly promotes the local heat transfer, leading to the elevated LHTC near the windward facade. Whereas, the local heat transfer is weakened by the wall jet, resulting in the lower LHTC on the leeward side.

In view of the analogous nature of the advection-diffusion equations it is our hypothesis that the heat and mass transfer in incompressible flow is similar to each other so the convective heat transfer over 2D ribs can be used to complement the pollutant removal in 2D idealized street canyons in order to shade some light on this fundamental urban air pollution problem.

METHODOLOGY

Two turbulence models are employed to compare the behaviours of wind and pollutant transport in idealized 2D street canyons of different ARs. Both the Reynolds-averaged Navier-Stokes (RANS) equations with the renormalization group (RNG) *k-ε* turbulence model and the large-eddy simulation (LES) with the one-equation subgrid-scale (SGS) model are used.

The commercial computational fluid dynamics (CFD) code FLUENT 6.3.26 (FLUENT, 2009) and the open source CFD code OpenFOAM 1.6 (OpenFOAM, 2009) are adopted, respectively, in the RANS model and the LES.

LES model description

The LES computational domain is shown in Figure 1a. Its height is 6*h* that consists of the leeward and the windward buildings of equal height *h*, and a shear layer of height 5*h* aloft. The shear layer extends *h*/2 horizontally over both the upstream and downstream buildings constructing a (repeated) unit of the 2D street canyon. The street width *b* between the leeward and the windward buildings is the sole parameter in the geometrical configuration (to vary the ARs). The spanwise extent of the domain is 5*h*. To consider the worst scenario from the pollution perspective, the prevalent wind, which is driven by the pressure gradient in the shear layer, is aligned perpendicular to the street axis. The homogeneous spanwise direction can then be averaged out in the three-dimensional computational domain forming an idealized 2D street canyon (Figure 1b).

LES boundary conditions

The LES is periodic in the horizontal directions representing the flow over infinitely long and infinitely repeating street canyons. The top of the domain is assumed to be shear free, while the solid boundaries are prescribed as no-slip conditions.

The pollutant concentration is constant (= C_0) on all solid boundaries, including the leeward and windward facades and roofs, as well as the streets. The upstream inflow is prescribed as pollutant free while the open-boundary condition is applied at the downstream outflow. In line with the flow field, the pollutant is assumed to be the periodic in the spanwise direction.

***k*-*ε* turbulence model description**

Unlike the LES, the computational domain in the *k*-*ε* turbulence model is 2D that consists of 13 identical 2D street canyons (Figure 1c). Same as the LES, the repeatable street canyon unit with building height *h* and street width *b* is assembled in the domain of height 6*h*. The domain is long enough so that the wind and turbulence are fully developed after the sixth street canyons (Garmory *et al.*, 2008). Thus, the seventh street canyon, which is the centre one, is the street canyon to be examined.

***k*-*ε* turbulence model boundary conditions**

The velocity at the domain inflow is given by the wind profile in the form of the power law

$$u(z) = U_0 \left(\frac{z}{6h} \right)^{\alpha} \qquad (1)$$

where U_0 (= 0.1753 ms^{-1}) is the free stream velocity, α (= 0.28) the wind profile exponent, and z the wall-normal distance measuring from the roof level. An open boundary is prescribed at the outflow and the domain top is assumed to be shear-free. Similar to the LES, no-slip conditions are prescribed on all the solid boundaries.

The pollutant source of constant concentration C_0 is placed at the street, facades and roof in the seventh street canyon (Figure 1c). Zero pollutant inflow is applied upstream while zero-gradient pollutant concentration is assumed at all other boundaries.

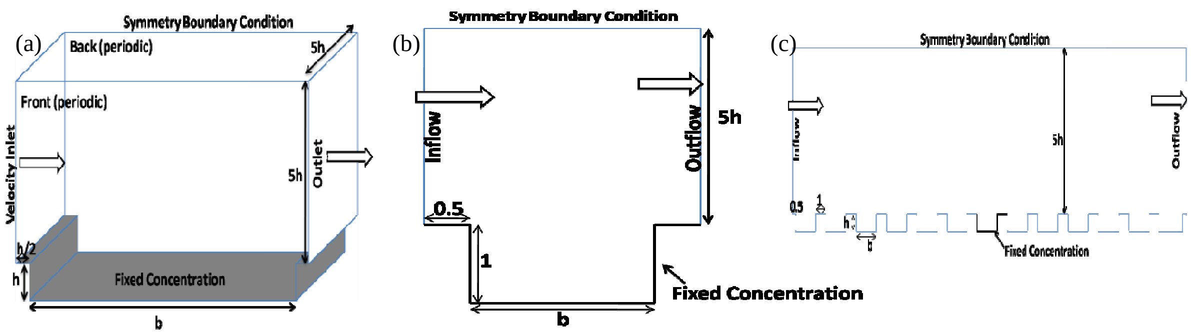

Figure 1. (a) Computation domain of the LES; (b) averaged two-dimensional computational domain in the LES; and (c) 13-street-canyon computational domain in the *k*-*ε* turbulence model

In this paper, the building height *h* is kept constant at 1 and the street width is varied (*b* = 15, 11, and 4) constructing the street canyons of ARs 0.0667, 0.0909, and 0.25.

Local heat/pollutant transfer coefficient (LHTC/LPTC)

The heat transfer is described by the convection-diffusion equation

$$\frac{\partial \bar{\theta}}{\partial t} + u_j \frac{\partial \bar{\theta}}{\partial x_j} = \alpha \frac{\partial^2 \bar{\theta}}{\partial x_j^2} \qquad (2)$$

where θ is the temperature, u the streamwise velocity and α the thermal diffusivity. Overlines represent the RANS-averaged quantities in *k*-*ε* turbulence model or the resolved scales in LES. Analogously, the mass (pollutant) transport equation is

$$\frac{\partial \bar{\phi}}{\partial t} + u_j \frac{\partial \bar{\phi}}{\partial x_j} = \kappa \frac{\partial^2 \bar{\phi}}{\partial x_j^2} \tag{3}$$

where ϕ is the mass (concentration) and κ the mass diffusivity. Given the similar mathematical model, the pollutant transport behaviours are expected to be the same as its heat transfer counterpart.

LHTC is defined as

$$LHTC = \left\langle \frac{q''}{\rho c_p} \right\rangle = \left\langle \overline{w}\,\overline{\theta} \right\rangle + \left\langle w''\theta'' \right\rangle + \left\langle \alpha \frac{\partial \theta}{\partial z} \right\rangle + \left\langle \alpha_{sgs} \frac{\partial \theta}{\partial z} \right\rangle. \tag{4}$$

Here, q'' is the heat flux, ρ the air density, and c_p the specific heat. Equation (4) consists of four terms: the mean component $\left\langle \overline{w}\,\overline{\theta} \right\rangle$, the fluctuation component $\left\langle w''\theta'' \right\rangle$, the molecular component $\left\langle \alpha \frac{\partial \theta}{\partial z} \right\rangle$ and the SGS component $\left\langle \alpha_{sgs} \frac{\partial \theta}{\partial z} \right\rangle$.

Likewise, the local mass (pollutant) transfer coefficient is defined in a equivalent manner

$$LPTC = \left\langle \overline{w}\,\overline{\phi} \right\rangle + \left\langle w''\phi'' \right\rangle + \left\langle \kappa \frac{\partial \phi}{\partial z} \right\rangle + \left\langle \kappa_{sgs} \frac{\partial \phi}{\partial z} \right\rangle. \tag{5}$$

It is noteworthy that the fluctuation and SGS components are excluded from the RANS calculation because of the *k-ε* turbulence model. The LES calculates explicitly most of the energy-carrying eddies according to the eddy size. As most near-wall eddies are small in size, the meshes are stretched toward the solid boundaries for more accurate turbulence calculation. While most eddies in the core of the computational domain are larger in size, coarser meshes are used to save computer resources. On the other hand, the *k-ε* turbulence model models all the turbulence in one single length scale, it is difficult to obtain a precise solution in the near wall-region without the modelling of small eddies. Consequently, the LES is expected to be more accurate than the *k-ε* turbulence model in general. The difference in the modelling results is reported below.

MODEL VALIDATION

The LPTC on the ground in the street canyon is calculated from the results of the LES and the *k-ε* turbulence models. The experimental results of Aliaga *et al* (1994) are used to validate the two models. It is noteworthy that a direct comparison among the experimental and modelling results is impossible because of the different Reynolds number (Re). A conversion of the LHTC in Aliaga *et al.* (1994), and the LPTC in the LES and RANS models to a dimensionless parameter, Nusselt number (Nu), is required. Two (ARs = 0.25 and 0.0909) out of the three aspect ratios are examined in the validation exercise.

Nu is the ratio of convective heat transfer to conductive heat transfer (Cengel 1998), i.e.

$$Nu_{Aliaga} = \frac{Hh}{k} = \frac{LHTC \times h}{k} \tag{6}$$

where h (= 0.025 m) is the characteristic (rib) height and k (= 0.026 W m^{-1} K^{-1}) the thermal conductivity in Aliaga *et al.* (1994). In the CFD, a transformation (Cengel 1998) is necessary that is defined as

$$Nu_{CFD} = \frac{Hh}{k} = \frac{Hh}{\rho c_p \alpha} = \frac{\rho c_p \, LPTC \times h}{\rho c_p \kappa} = \frac{LPTC \times h}{\kappa}. \tag{7}$$

Here, h (= 1 m) is the building height and κ (= ν/Sc) the mass diffusivity. Sc (=0.72) is the Schmidt number in the two models, while the kinematic viscosity v is 10^{-5} m^2 s^{-1} and 1.7894×10^{-5} m^2 s^{-1}, respectively, in the LES and the *k-ε* turbulence models.

In view of the different Re employed in the CFDs and the experiment (Aliaga *et al.*, 1994), the empirical correlation

$$Nu = C \, \mathrm{Re}^m \, \mathrm{Pr}^n \tag{8}$$

for flow over a flat plate, where C, n, Pr (= 0.72), and m (assumed to be 4/5) are constants. Although the Reynolds number is different, the LHTCs in Aliaga *et al.* (1994) and in the two CFDs are expected to fulfil the following empirical correlation

$$Nu_{CFD} = \left(\frac{\mathrm{Re}_{CFD}}{\mathrm{Re}_{Aliaga}} \right)^{4/5} Nu_{Aliaga} = \left(\frac{U_{CFD}}{U_{Aliaga}} \times \frac{h_{CFD}}{h_{Aliaga}} \right)^{4/5} Nu_{Aliaga} \tag{9}$$

where U_{CFD} and U_{Aliaga} are, respectively, the free-stream velocities in the CFDs and in the experiment (Aliaga *et al.*, 1994). h_{CFD} (= 1m) is building height in the CFDs and h_{Aliaga}(= 0.025m) is the rib height in the experiment.
Correction has been implemented by scaling the experimental Nu to the numerical ones according to Equation (2). As shown in Figure 2, the LPTC determined in the LES agrees well with the experimental value. Whereas, the LPTC calculated by the

(a) (b)

k-ε turbulence model exhibits a discrepancy compared with the LES and experimental data. In the street canyon of AR = 0.0909 (Figure 2a), the LES and *k-ε* turbulence models agree equally well with the experimental solution. On the other hand, in AR = 0.25 (Figure 2b), a large discrepancy is observed when comparing the LPTC calculated by the *k-ε* turbulence models with the LES and experimental values, especially at the centre of the street. This difference is mainly attributed to the high turbulence level induced in the street centre and the single-length scale employed in the *k-ε* turbulence model.

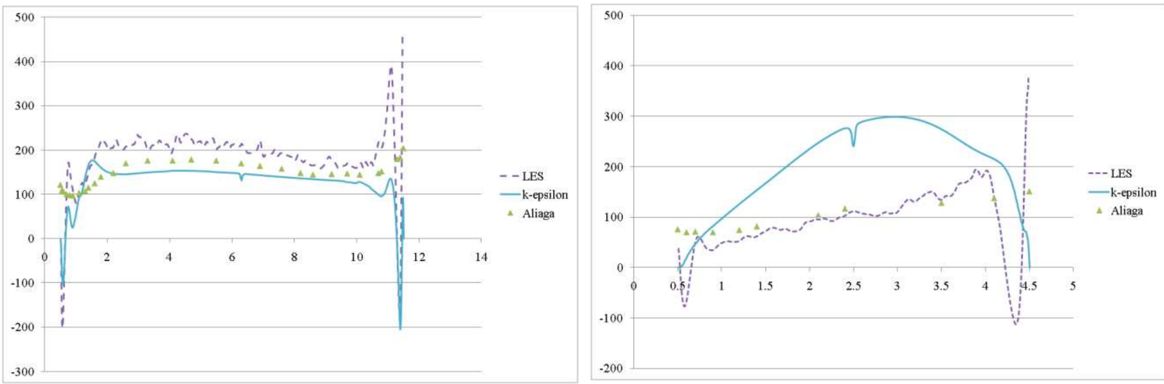

Figure 2. Comparison between the experimental and numerical solutions in AR =: (a) 0.0909 and (b) 0.25

RESULTS AND DISCUSSION

As demonstrated in the previous section, the LES solution is more reliable for the calculation of the LHTC in street canyons. Hence, only the LES results will be discussed in the following sections. Figure 3 shows the flow characteristics and the LPTC simultaneously in the street canyons of ARs = 0.0667, 0.0909, and 0.25.

In the isolated roughness regime (ARs = 0.0667 and 0.0909), the prevalent flow passes over the leeward building, separates at the roof-level leeward corner, entrains down into the street canyon, and finally touches down at the reattachment point on the street. The entrainment air stream diverges into two parts in the near-ground region. The reverse flow develops the wall jet towards the leeward side while the downstream flow develops the boundary layers on the windward side. The peak LPTC coincides with the reattachment point. The wall jet bends upward along the leeward facade leading to the primary recirculation near the leeward building. At the same time, the downstream boundary layer continues to flow along the street until the separated region. The flow leaves the street after the separation point, travels through the windward roof, and moves to the next street canyon. This flow binds the air in the windward side. Moreover, due to the interface boundary condition between two fluids, the airflow circulates forming another clockwise-rotating primary recirculation. This second primary recirculating flow impinges on the lower windward facade developing the upstream boundary layer. The impingement contributes to the second maximum LPTC. The LPTC decreases thereafter because of the boundary layer until it arrives at the trough of LPTC at the separated region. The rapid increases in the LPTC in the primary recirculations on the leeward and windward sides lead to the abrupt changes in pollutant removal performance. The gentle decrease of the LPTC associates with the gradual decrease of the pollutant removal rate in the redevelopment region with the main air stream flow. For a better urban planning, the pollutant emission sources, such as traffic roads with vehicular emission and domestic exhaust pipes, should be built in the redevelopment region, preferably near the reattachment region. The air pollutant will then be removed more efficiently.

In the wake interference regime (AR = 0.25), the prevalent wind in the shear layer tends to flow downward after separation at the leeward building. However, the narrow street is not wide enough for the separated flow entraining down into the street level but leaves the street canyon instead. Hence, the reattachment and separation regions are vanished in this regime and are replaced by one primary recirculation. The wind trapped inside the street canyon rotates in a clockwise direction due to the wind shear along the roof-level interface that impinges the ground near the ground-level windward corner. The flow impingement initiates the maximum LPTC on the windward side while the upstream-flowing wall jet suppresses the LPTC. The collective effect turn out develops the monotonic increasing LPTC from the leeward side to the windward side. To facilitate air pollutant removal, emission sources should be placed on the windward side when the street is narrow, say AR less than 5, to enjoy the better pollutant removal on the windward side.

Apart from the LPTC along the ground surface, the mechanisms of pollutant removal via the roof level are also analyzed. In the isolated roughness regime (ARs = 0.0667 and 0.0909), the prevalent air stream from the inflow separated at the leeward building is able to entrain down to the street within the wider street canyon, the pollutant is then carried away from the street canyon across the roof by the wind. The pollutant removal is mainly governed by the fresh air entrainment from the shear layer down into the street canyons.

While in the wake interference regime (AR = 0.25), turbulent dispersion is the dominated mechanism for the pollutant removal. Owing to the isolated primary recirculation in the street, the weak fresh air entrainment is insufficient to remove the air pollutant from the street canyons. Instead, the primary recirculation inside the street canyon carries part of the air pollutants from the street level upward to roof level by the mean flow, which is then passed across the roof by turbulent dispersion.

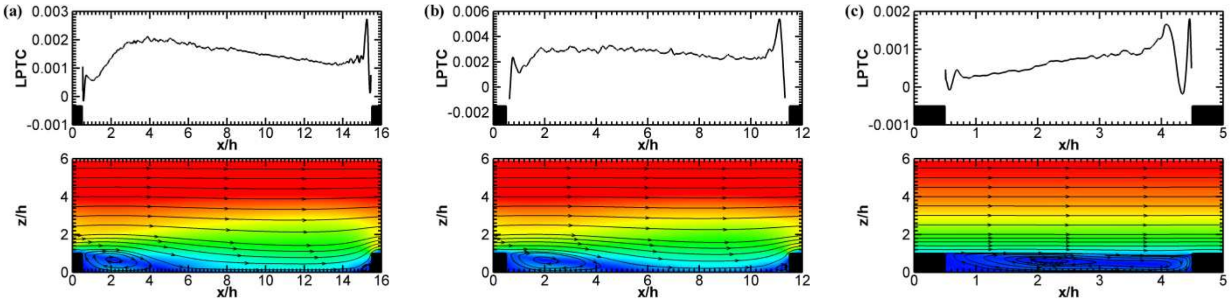

Figure 3. The relationship between the LPTC and characteristic flow regimes, AR = (a) 0.0667; (b) 0.0909; and 0.25.

CONCLUSIONS

Both the Reynolds-averaged Navier-Stokes (RANS) equations with the renormalization group (RNG) k-ε turbulence model and the large-eddy simulation (LES) with the one-equation subgrid-scale (SGS) model are applied to simulate the wind and pollutant transport in idealized two-dimensional (2D) street canyons of aspect ratios (ARs) 0.0667, 0.0909, and 0.25. A model validation is performed for the street canyons of ARs 0.0909 and 0.25 by comparing the Nusselt number with the experimental data from Aliaga *et al.* (1994). The LES results show more consistent results with the experimental ones; and hence more accurate. The relationship between the flow characteristics and the local pollutant transfer coefficient (LPTC) is examined for the isolated roughness and wake interference regimes. In the isolated roughness regime, the maximum and minimum LPTC are tightly coupled, respectively, with the reattachment and separation points. While in the wake interference regime, the single isolated recirculation results in the monotonically increasing LPTC from the leeward side to the windward side. The roof-level pollutant removal mechanisms are also investigated. The fresh air entrainment from the shear layer down into the street canyons is the major mechanism removing the pollutant in the isolated roughness regime, while the turbulent diffusion is found to be the dominated mechanism for pollutant removal in the roof level. To improve the air quality, the LPTC could be used as a reference that the pollutant emission sources should be placed somewhere with the relatively larger LPTC. To earn a more comprehensive understanding, the skimming flow regime should also be taken into account and more ARs in the isolated roughness and the wake interference regimes should be studied in future investigations.

ACKNOWLEDGEMENTS

This project is partly supported by the General Research Fund of the Hong Kong Research Grant Council HKU 715209E.

REFERENCES

Acharya, S., Dutta, S., Myrum, T.A. and Baker, R.S., 1993: Periodically developed flow and heat transfer in a ribbed dust: *Int. J. Heat Mass Transfer*, **36(8)**, 2069-2082.

Aliaga, D.A., Lamb, J.P. and Klein, D.E., 1994: Convection heat transfer distributions over plates with square ribs from infrared thermography measurements: *Int. J. Heat Mass Transfer*, **37(3)**, 363-374.

Barlow, J.F., Harman, I.N. and Belcher, S.E., 2004: Scalar fluxes from urban street canyons. Part I: Laboratory simulation: *Boundary-Layer Meteorology*, **113**, 369-385.

Berkowicz, R., Ketzel, M., Vachon, G., Louka, P., Rosant, J.-M., Mestayer, P.G. and Sini, J.-F., 2002: Examination of traffic pollution distribution in a street canyon using the Nante'99 experimental data and comparison with model results: *Water, Air, and Soil Pollution: Focus*, **2**, 311-324.

Cengel, Y.A., 1998: Heat transfer: A practical approach, *McGraw-Hill*, USA, 357-359 pp.

FLUENT, 2009: http://www.fluent.com/.

Garmory, A., Kim, I.S., Britter, R.E. and Mastorakos, E., 2008: Simulations of the dispersion of reactive pollutants in a street canyon, considering different chemical mechanisms and micromixing: *Atmospheric Environment*, **43(31)**,4670-4680.

Hishida, M., 1996: Local heat transfer coefficient distribution on a ribbed surface: *Journal of Enhanced Heat Transfer*, **3(3)**, 187-200.

Letzel, M.O., Krane, M. and Raasch, S., 2008: High resolution urban large-eddy simulation studies from street canyon to neighbourhood scale: *Atmospheric Environment*, **42**, 8770-8784.

Liou, T.-M., Hwang, J.-J. and Chen, S.-H., 1993: Simulation and measurement of enhanced turbulent heat transfer in a channel with periodic ribs on one principal wall: *Int. J. Heat Mass Transfer*, **36(2)**, 507-517.

Oke, T.R., 1988: Street design and urban canopy layer climate: *Energy and Buildings*, **11(1-3)**, 103-113.

OpenFOAM, 2009: http://www.openfoam.com/.

WHO Regional Office for Europe Air Quality and Health Programme, 2007: How large a risk to health is air pollution in the European Region, and is there evidence indicating effective measures to reduce it?